

Hot corrosion behavior of dense CYSZ/YSZ bilayer coatings deposited by atmospheric plasma spray in Na₂SO₄+V₂O₅ molten salts

Abstract

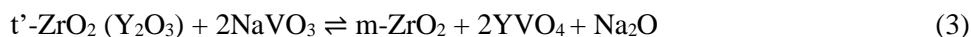
In this work, the hot corrosion (HC) resistance of bilayer thermal barrier coatings (TBC) composed of dense Ceria-Yttria Stabilized Zirconia (D-CYSZ) and Yttria-Stabilized Zirconia (YSZ) deposited using the atmospheric plasma spray (APS) technique was evaluated. Two kinds of HC tests were performed using different salt concentrations and thermal cycling (adding fresh salt between cycles) with a constant salt mixture (Na₂SO₄-V₂O₅) and constant testing temperature (900°C). The results showed that the HC mechanism changes with the testing procedure and the outer D-CYSZ layer acts as a barrier to protect the inner layers against HC degradation, although the formation of vertical cracks during the coating deposition process affected the corrosion resistance of the TBC systems.

1. Introduction

Thermal barrier coatings (TBCs) are used to protect parts exposed to the highest operating temperatures in industrial gas turbines (IGTs), allowing operating temperatures above the inherent capacity of the metallic substrates and thus enhancing turbine efficiency during operation. The parts to be protected are mainly those located on the hot gas path, including the combustor chamber, liners, first stage stationary and rotating blades, and seals [1–4].

The Top Coat (TC) layer most used as a thermal insulator is Yttria-Stabilized Zirconia containing 7–8 wt.% of yttria in solid solution (7YSZ). This amount of yttria stabilizes the non-transformable tetragonal phase (t') of zirconia at room temperature, meaning it does not undergo the martensitic transformation to the monoclinic phase during cooling [1,5]. This phase possesses a high thermal expansion coefficient (10.5–11.5 × 10⁻⁶ K⁻¹), high toughness, and low thermal conductivity (i.e., 1.2 and 1.8 Wm⁻¹K⁻¹) [6–10] when compared to the monoclinic structure.

When an IGT operates with low-quality liquid fuels containing high amounts of impurities such as sodium (Na), vanadium (V), and sulfur (S), these might form salts with strong acid-base properties during combustion, *e.g.*, sodium sulfate (Na₂SO₄), vanadium pentoxide (V₂O₅), and sodium vanadate (NaVO₃) [11]. These molten salts infiltrate through any TBC defects (i.e., pores and cracks) and react mainly with the Y₂O₃ phase, promoting the destabilization of the t'-phase [12–14]. This failure mechanism is called salt-induced hot corrosion (HC) attack, the main reactions between the molten salts and YSZ being as follows [13]:



Equations 1 to 3 describe reactions with a Lewis acid-base nature and the fluxing (dissolution) of the 7YSZ in the molten salt. These synergistic interactions generate depletion of the Y₂O₃ phase content in the 7YSZ solid solution, promoting the destabilization of t'-YSZ to form m-ZrO₂; this phase

transformation involves a 3–5% volumetric expansion and formation of yttrium orthovanadate (YVO_4) along the infiltration path through the TBC thickness, generating stress, cracking and subsequent delamination of the YSZ layer [14–16].

One way to counter the accelerated degradation generated by HC attack is to design multimaterial multilayered TBC architectures that can slow down the infiltration of salts and even promote their self-healing during service. These TBC architectures might include bilayer structures, densified vertical cracking overlays, and functionally graded structures [17–21]. Laser glazing treatments have also been employed to modify the TC surface [22–24], and alternative materials with higher HC resistance to molten salts like $\text{La}_2\text{Zr}_2\text{O}_7$ [25], $\text{Sm}_2\text{Zr}_2\text{O}_7$ [26], $\text{Gd}_2\text{Zr}_2\text{O}_7$ [27–29], and ZrO_2 stabilized and co-stabilized with In_2O_3 , Sc_2O_3 , or Ta_2O_5 [16,30–33] have been tested.

Ceria-Yttria Stabilized Zirconia (CYSZ) is a good TC candidate for TBC systems due to its higher thermal expansion coefficient and good thermal shock resistance, lower thermal conductivity, and greater stability in comparison to 7YSZ [9]. Moreover, CYSZ has shown outstanding resistance to molten salt attack [34–38] because the cerium oxide (CeO_2) acts as a stabilizer of the t' -phase of zirconia and exhibits better resistance to salt-induced HC due to its higher acidity compared to Y_2O_3 , which reduces the reactivity of the TC with the molten salts [39].

This work studies four different TBC architectures composed of dense CYSZ (D-CYSZ) and porous 7YSZ layers, which were exposed to two different HC conditions. The degradation of the coatings due to HC was investigated and correlated with the microstructural, chemical and morphological changes observed in the samples.

2. Materials and methods

2.1. Coating deposition

An Sinplex pro-gun (*Oerlikon Metco, USA*) was used to deposit the D-CYSZ/YSZ systems onto Inconel 625 disks ($\text{Ø}25.4 \times 5$ mm) by atmospheric plasma spray (APS) in the facilities of Empresas Publicas de Medellín, Colombia (EPM). Figure 1 illustrates the four multilayered TBC architectures deposited, in which the thickness of the outer D-CYSZ layer was designed to be 50, 100 or 150 μm , maintaining a total thickness of the TC of 300 μm . All Top Coat (TC) architectures had a high-toughness, low-porosity YSZ (LP-YSZ) layer with a thickness of about 50 μm between the BC and the porous YSZ layer, which has proven effective at enhancing the thermomechanical resistance of the system [40–42].

Amdry 386-2.5, Metco 204NS-G, and 205NS (*Oerlikon Metco*) powders were used as feedstock material for the NiCoCrAlY bond coat, and YSZ and CYSZ as the TC layers, respectively.

Before the spraying process, Inconel 625 substrates were grit-blasted with alumina particles (F24 grain size: 600–850 μm), cleaned ultrasonically for 3 minutes with isopropyl alcohol, and dried in cold air. The samples were then pre-heated at approximately 160 °C before spraying each layer. The spray parameters of each layer had previously been optimized, and the best conditions are summarized in Table 1.

2.2. Hot corrosion tests

The HC tests were performed using high-purity Na₂SO₄ (*JT Baker*) and V₂O₅ (*Aldrich chemistry*) powders in a mixture of 32 wt.% of Na₂SO₄ and 68 wt.% V₂O₅ at the CIDESI facilities in Queretaro, Mexico. The mixture was spread over the surface of the samples, avoiding the edges. The D-CYSZ/YSZ TBC architectures were evaluated following the methodology reported in [11,42] in triplicate for each test, using two different HC tests as described below.

HC-concentration test: The salt deposit concentration was set to 1, 3, and 5 wt.% of the total weight of the TC, which was previously determined in detached coatings. Samples were covered with the salt deposit, heated up to 900°C, and held for 10 hours in air atmosphere inside the oven.

HC-cyclic test: The samples were exposed to a salt deposit with a concentration of 1 wt.% and then treated at 900 °C for 10 hours to complete one cycle. Then, the samples were cooled down to room temperature, and a fresh salt mixture was added (1 wt.%) over the sample and exposed to the next cycle. The process was repeated until the tetragonal-phase percentage decreased to 10 wt.% or less.

2.3. Coating characterization

Microstructural characterization of the CYSZ/YSZ TBC architectures was conducted in the Tribology and Surface group facilities in Medellín, Colombia and the CPT Thermal Spray Center in Barcelona, Spain according to ASTM E1920 and ASTM E2109 standards, using an eclipse LV1000 (Nikon, Japan) optical microscope (LOM) equipped with a Nikon DS-2Mv digital camera. Morphological characterization was carried out using a JEOL (Japan) JSM-5910LV scanning electron microscope (SEM). Chemical characterization was carried out using Energy Dispersive Spectroscopy (EDS) with a Pentafet 7324 detector (Oxford Instruments, UK), operating at 133eV (nominal area 10 mm²) with an ATW2 window.

A Rigaku (Japan) Smart Lab X-Ray diffractometer (XRD) was used for the structural characterization of the samples before and after the HC attack in the CIDESI facilities in Queretaro, Mexico. A Bragg Brentano geometry with Cu- α radiation ($\lambda=1.5406 \text{ \AA}$) and measurement range from 20 to 80° with steps of 0.01° were the parameters used to collect the diffractograms. Rietveld analysis was carried out with the aid of the GSAS software, using Chebyshev polynomials with eight terms and the Pseudo-Voigt and asymmetry function to fit the background and the peak profiles respectively, obtaining Chi² values below 3.3. The following data were used for quantitative analyses:

- Tetragonal phase with yttria contents of 8 mol.% YO_{1.5}: t'-YSZ (ICOD 01-082-1241)
- Tetragonal phase with yttria contents of 4 mol.% YO_{1.5}: t-YSZ (ICOD 01-078-1808)
- Monoclinic phase: *m*-ZrO₂ (ICOD 01-078-0047)
- Cerium oxide phase: CeO₂ (ICSD 98-018-0851)
- Yttrium orthovanadate phase: YVO₄ (ICOD 01-074-11-72)

Structural analysis of the TC was performed using a μ -Raman spectroscope (Horiba LabRAM HR Evolution, Japan) equipped with a 532 nm Ar laser and Olympus microscope using a 50x objective, in the facilities of the Universidad Nacional Medellín, Colombia. Spectra were taken every 50 μm until reaching the BC in the range from 120 to 200 cm⁻¹ with an acquisition time of 5 seconds.

3. Results

3.1. Microstructure of D-CYSZ/YSZ bilayer coatings

Table 2 shows the thickness of the APS-deposited YSZ and D-CYSZ layers, which were intended to be as close as possible to the architectures defined in Figure 1. The thickness of the BC and LP-YSZ layers was kept constant for all TBC architectures and is shown in Table 2. The average porosity of the YSZ layers of the different architectures was 15.9 ± 1.6 % and that of the LP-YSZ layers was 6.0 ± 1.3 %. The layers included globular pores that can be classified as large (>16 μm), medium (6–16 μm) and fine (1–6 μm) [43], and a high density of inter- and intra-splat cracks with high interconnectivity, as shown in Figure 2.

Table 2. Thickness of the layers of the TBC systems studied

The average porosity of the outer D-CYSZ layer of the three CYSZ systems was 5.1 ± 1.2 %, with a high density of fine globular pores and intra-splat cracks. This layer also presented vertical cracks with a density of 4.3 cracks/mm for the CYSZ50 sample, 3.9 cracks/mm for the CYSZ100 sample, and 3.2 cracks/mm for the CYSZ150 sample. During the pre-heating and spraying processes, heat transfer led to differential thermal expansion of the D-CYSZ and YSZ layers, due to their dissimilar thermal expansion coefficients [9,44]. This differential thermal expansion leads to biaxial stresses in the D-CYSZ layer, which, together with the splat boundaries, constitute preferential paths for vertical crack growth with further temperature changes [45,46].

3.2. Hot corrosion resistance

3.2.1. Analysis of microstructural changes in the TBC systems

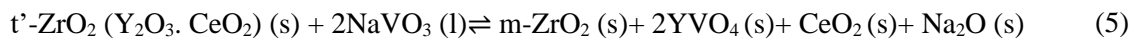
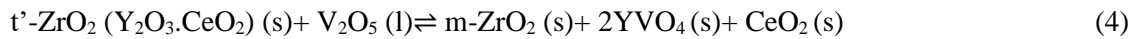
Figure 3 compares the X-ray diffractograms of the multilayer systems before and after HC attack under different conditions.

A reduction in the intensity of the (101) and (011) main peaks corresponding to the tetragonal phases ($2\theta=30.1^\circ$ for YSZ and $2\theta=29.9^\circ$ for CYSZ), combined with an increase in the intensity of the YVO_4 , CeO_2 , and m-ZrO_2 peaks were observed after HC attack. In the HC-concentration tests, an increase in salt concentration accelerated the tetragonal-to-monoclinic phase transformation, as demonstrated by the high intensity of the m-ZrO_2 main peaks ($2\theta=28^\circ$ and 31.5°), as well as the emergence of new peaks in this phase at $2\theta=24^\circ$ and 24.4° . These transformations occurred because more salt was available to interact with the stabilizing compounds (Y_2O_3 and CeO_2), which increased the amount of

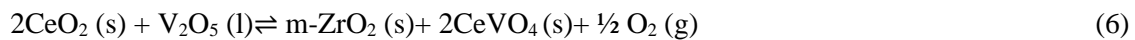
HC products as demonstrated by the higher intensity of the YVO_4 ($2\theta=24.9^\circ$) and CeO_2 ($2\theta=28.5^\circ$) peaks when the salt concentration was increased.

HC-cycle tests also showed a progressive decrease in the intensity of the peaks in the tetragonal phases of the YSZ and CYSZ systems (Figure 3b), combined with an increase in the intensities of the peaks of the YVO_4 , CeO_2 , and $m-ZrO_2$ phases as a function of the number of cycles. HC-cycle tests showed more extensive destabilization of the YSZ system than the CYSZ architectures after each cycle, indicating the higher resistance of the D-CYSZ layer to HC attack.

CeO_2 is considered a precipitation byproduct that results from the so-called mineralization process described by Jones [14], according to which exposure to molten salts contributes to the formation of the stable phases predicted by the ZrO_2 - CeO_2 equilibrium diagram at the temperature of interest, i.e., monoclinic zirconia and free CeO_2 particles for the 700–900°C range. This destabilization of tetragonal zirconia was previously reported by Park et al. [34] in CYSZ coatings exposed to a V_2O_5 - Na_2SO_4 salt mixture. Based on the experimental evidence observed in this work and the existing literature [13,14,47–49], a summary of the expected reactions occurring in zirconia in the presence of molten vanadium-rich salts is as follows:



Reidy and Jones reported that the formation of $CeVO_4$ requires an increase in the chemical activity of V_2O_5 in the melt for the chemical reaction described by equation 6 to occur [47]. However, in this work, no HC products associated with cerium, including cerium orthovanadate ($CeVO_4$), were found after the XRD analyses of the samples studied.



Previous results by the authors [11] showed that in a Na_2SO_4 - V_2O_5 salt mixture, the V_2O_5 activity is proportional to SO_3 partial pressure, which is low when the experiment is performed in air. Moreover, a higher concentration of Na_2SO_4 decreases the melt's acidity. The high acidity of ceria compared with yttria [13,48] favors the formation of YVO_4 in CYSZ systems, which generates a preference for the molten salts to react with the co-stabilizing element. Therefore, the HC attack mechanism of the CYSZ layers is dominated by the mineralization (CeO_2 precipitation) and formation of YVO_4 .

Figure 4 presents the tetragonal phase content after HC tests for the TBC systems studied. A reduction in the content of the tetragonal phases (t' -YSZ, t -YSZ and t' -CYSZ) with the increase in salt concentration and cycles is shown. In YSZ samples, the t' -YSZ phase disappeared when the salt concentration used was 5 wt.% in HC-concentration tests, or after four cycles in the HC-cycle tests. The protection provided by the D-CYSZ layer is evident given that, for any testing condition, the amount of tetragonal phase in CYSZ samples was always higher than in the YSZ samples.

Phase quantification of the HC products is illustrated in Figure 5. The amount of HC products increased with salt concentration (Figure 6a), obtaining values of up to 50 wt.% for the YSZ sample, which is consistent with the results shown in Figures 3 and 4. Figure 5b shows that the amount of YVO_4 increased linearly with the number of cycles for the YSZ system, whereas in the CYSZ systems, the CeO_2 remained stable with the number of cycles with a slight downward trend.

To summarize the above results, Table 3 shows the phase quantification of the systems studied after the HC tests (HC-concentration and HC-cycle tests).

3.2.2. Analysis of corroded surfaces and HC products

HC-concentration tests

The surface of the YSZ and CYSZ TBC architectures submitted to HC-concentration tests is presented in Figure 6. The YSZ system (Figure 6a) exhibited an evident TC peel off at the edges, which was not observed in CYSZ systems (Figures 6b). In the YSZ system, the HC products observed had rod-like and needle-like morphologies characteristic of YVO_4 crystals. On the other hand, the surface of CYSZ systems (Figure 6b) comprised rods held together with cubic and semi-cubic crystals and "free" cubic and semi-cubic crystals.

Figures 6c and 6d show the surface view of the YSZ and CYSZ TBC architectures tested with 5 wt.% of salt. It is important to note that similar results were observed for all CYSZ architectures. The D-CYSZ layer was delaminated above 20% in the CYSZ architectures, whereas only coating spallation and delamination at the samples' edges were observed in the YSZ architecture. This salt concentration produced severe HC attack on the tested TBC architectures, generating failure at both interfaces and within the layers that comprise the coating system. The YSZ system had a YVO_4 phase predominantly with rod-like morphology and some needle-like particles as well (Figure 6c).

On the other hand, the HC products for all CYSZ systems (Figure 6d) exhibited a rod-like morphology (YVO_4 phase) mixed with cubic and semi-cubic crystals (CeO_2 phase) that were larger compared with the samples tested at 3 wt.% salt concentration, which correlates well with the trend observed after the quantitative Rietveld analysis presented in Figure 5a. The elemental analysis shown in Figure 6e confirmed the presence of V and Y in the rod-like particles and Ce and O₂ in the cubic and semi-cubic crystals. The back-side of the spalled D-CYSZ layers was also studied to analyze the coating's failure. Figure 7 shows the surface of the D-CYSZ/YSZ interface and the corresponding EDS analyses.

The analysis revealed the characteristic morphologies of the HC products, i.e., cuboidal crystals (Figure 7a) of the CeO_2 phase and characteristic rod-like morphology of the YVO_4 phase (Figure 7b). These results are consistent with the results of studies by Jones [14], Daroonpavar et al. [15], Park et al. [34], and Levi et al. [50], among others, in which the corrosion products formed at the coating's defects, decreasing the compliance and generating mechanical stresses that promote cracking and delamination of the coating.

HC-cycle tests

Figure 8 shows the HC products at the surface of the multilayer systems after the HC-cycle tests. No visible coating spallation was observed in the samples after five cycles, even at a salt concentration of 5 wt.% and once the complete destabilization of the tetragonal phases had occurred. SEM images of the YSZ architecture revealed the existence of needle-type YVO_4 crystals (Figure 8a). A comparison of the results with those corresponding to the HC-concentration test (see Figure 6), when the samples (cycles and concentration) were exposed to the same salt concentration (5 wt.%), showed that YVO_4 crystals growing under cyclic conditions are more numerous and have a larger length-to-width ratio than those growing under isothermal conditions. A similar situation was observed in CYSZ systems, in which the HC products have needle-like morphology growing uniformly across the entire surface (Figure 8b) and some cubic and semi-cubic CeO_2 crystals, confirming the results of the XRD analyses (Figure 5b). These results suggest that changing HC corrosion tests' parameters promotes different growth kinetics of the corrosion products, which directly affects their morphology and size.

3.2.3. Analysis of LP-YSZ/YSZ interface

Figure 9 shows the BC/YSZ interface after HC-concentration tests with 5 wt.% salt concentration (Figure 9a) and five HC-cycle tests (Figure 9b). In both HC tests, the infiltration of the molten salt through the TC was evident. This accelerated BC degradation in different areas, resulting in heterogeneous growth of the TGO along the interface. It also resulted in Al depletion in the BC at the BC/YSZ interface and, therefore, reduced the amount of β precipitates when a thicker TGO was formed. The EDS spectra show the presence of vanadium in the TGO, which promotes coating failure. This result confirms that the D-CYSZ layer did not offer effective protection against molten salt penetration under the aggressive HC test conditions studied in this work, due to the presence of vertical cracks that allow the penetration of molten salts.

4. Discussion

The results presented above demonstrate that 5 wt.% salt concentration (HC-concentration test) and five cycles (HC-cycle test) were the most aggressive HC conditions tested in this work, as the X-ray diffractograms showed greater phase destabilization of the tetragonal phases (t' -YSZ, t -YSZ, and t' -CYSZ). These test conditions also generated a greater amount of HC products as confirmed by the phase quantification results and the SEM examination of the corroded surfaces. However, after five cycles, no coating detachment was observed in the CYSZ systems, as shown in Figure 10a. Observation of the microstructure in the bilayer systems after the HC-cycle test revealed areas where the YSZ system presented severe cracking without delamination or spallation, as well as reduced porosity throughout the thickness, which was also observed in the YSZ layers of CYSZ systems. It was found that the vertical cracks in D-CYSZ layers were infiltrated with products of the corrosion reactions without delamination. The change in the bilayer microstructure is produced by the fluxing

(dissolution) of the coating due to its reaction with the salts [12] and solidification of the molten salts and formation of HC products in the coating defects [15].

The Raman analysis of the cross-section of the YSZ system shows the characteristic peaks of m-ZrO₂ and YVO₄ phases at the surface and throughout the thickness of the coating (Figure 10b). This is consistent with the X-ray diffraction results, where the surface has a destabilization of the tetragonal phase of less than 10% (Figure 4). The intensities decrease close to the BC, where the vibration at 148 cm⁻¹ of the tetragonal phase is observed [51,52] due to the higher density of the LP-YSZ layer. Despite the infiltration of salts, the dissolution reactions were less aggressive in such a dense layer. The CYSZ systems presented higher phase destabilization at the surface due to the dissolution produced by the molten salts (as inferred from the XRD results). However, no phase transformation was observed inside the D-CYSZ layer in any of the samples studied, since they presented peaks corresponding only to the tetragonal phase (t'-CYSZ). Moreover, the YSZ layers of the CYSZ systems did not present peaks corresponding to HC products at 158 cm⁻¹ [51] as observed in the YSZ system, and systems with a D-CYSZ layer with a thickness above 100 μm showed vibrations in the tetragonal phase (t'-YSZ), indicating that the D-CYSZ layers offered protection against attack by molten salts despite the infiltration of molten salt, because the dissolution and formation of HC products were less aggressive.

Cross-sections shown in Figure 11a confirm the occurrence of delamination and spallation at the surface of the systems tested under 5 wt. % HC concentration (as observed in surface photos of Figure 6c and 6d). All samples showed several microstructure changes, even in areas where the TBC system did not fail. Delamination in the YSZ system was observed close to the LP-YSZ/YSZ interface. On the other hand, the bilayer systems presented delamination in the D-CYSZ layer and infiltration of vertical cracks with HC products, as shown in Figure 11b. The EDS spectrum confirmed the presence of Y and V in the gray areas within the vertical cracks, indicating a preference to form YVO₄ crystals in the D-CYSZ layer. These cracks allowed the penetration of the molten salts through the coatings.

The HC-cycle test was less aggressive than the HC-concentration test for the same salt concentration. The "stagnation effect" of the HC attack in the TBC system could be responsible for this behavior, given that similar results have been observed in HC tests in NiCoCrAlY alloys [53]. Replenishing with fresh salt every cycle during the test produces changes in the molten salts' surface and chemistry deposited in the coating, possibly decreasing the HC reaction's kinetics. This effect was demonstrated by the change in the morphology of the YVO₄ crystals (Figures 7 and 9), which are highly susceptible to the precursors' composition [54]. Moreover, the infiltration of cracks and pores with the early HC products (with high melting points) slows down the intake of new molten salt in the subsequent cycles, avoiding new reactions and generating more HC products within the coating.

Conclusions

This work showed that for CYSZ/YSZ TBC systems, the predominant HC mechanisms are dissolution (fluxing) and mineralization, which produce YVO₄ and CeO₂ crystals together with the

stabilization of monoclinic zirconia. A dense CYSZ layer with a thickness between 100 and 150 μm applied onto a YSZ coating acts a barrier to molten salts' attack, increasing the HC resistance of the TBC system. However, vertical cracks formed during the coating deposition process reduce the HC resistance of the TBC system.

HC test results showed that phase transformations (tetragonal to monoclinic) and the formation of HC products at the interfaces and defects have a high influence on the spallation and delamination of the coatings of the TBC system. These results were verified experimentally with the X-ray diffraction results and the corrosion products found in the detached layers' back-side.

The choice of HC test has relevant effects on the magnitude of damage in the TBC system. Isothermal exposure to a fixed amount of salts (HC-concentration tests) is more aggressive than the progressive addition of the salts (HC-cycle tests) because the latter does not allow the system to stabilize, retarding the reaction kinetics.

Acknowledgments

The authors gratefully acknowledge the financial support from *Empresas Públicas de Medellín- EPM*. The authors also thank CONACYT (FORDECYT 277265 project), CONMAD Consortium, and Thermal Spray Center-CPT of University of Barcelona for technical and financial support (2017SGR 01777 project).